

On the optimization of discrepancy measures

François Clément^{*1}, Nathan Kirk^{†2}, Art B. Owen^{‡3}, and T.
Konstantin Rusch^{§4,5,6}

¹Department of Mathematics, University of Washington

²Department of Applied Mathematics, Illinois Institute of
Technology

³Department of Statistics, Stanford University

⁴ELLIS Institute Tübingen

⁵Max Planck Institute for Intelligent Systems

⁶Tübingen AI Center

Abstract

Points in the unit cube with low discrepancy can be constructed using algebra or, more recently, by direct computational optimization. The usual L_∞ star discrepancy is a poor criterion for this because it is computationally expensive and lacks differentiability. Its usual replacement, the L_2 star discrepancy, is smooth but exhibits other pathologies shown by J. Matoušek. In an attempt to address these problems, we introduce the *average squared discrepancy* which averages over 2^d versions of the L_2 star discrepancy anchored in the different vertices of $[0, 1]^d$. Not only can this criterion be computed in $O(dn^2)$ time, like the L_2 star discrepancy, but also we show that it is equivalent to a weighted symmetric L_2 criterion of Hickernell's by a constant factor. We compare this criterion with a wide range of traditional discrepancy measures, and show that only the average squared discrepancy avoids the problems raised by Matoušek. Furthermore, we present a comprehensive numerical study that reinforces the advantages of the average squared discrepancy over other classical discrepancy measures, whereas the converse does not hold.

1 Introduction

Placing n points in $[0, 1]^d$ to minimize measures of discrepancy, i.e. as uniformly as possible, has been a fundamental challenge since the early 20th century [31,

^{*}fclement@uw.edu

[†]Corresponding author: nkirk@illinoistech.edu

[‡]owen@stanford.edu

[§]tkrusch@tue.ellis.eu

32, 34, 35]. The resulting low-discrepancy point sets are most commonly used in multivariate integration [8, 13, 26], but have application in computer graphics [17], neural network training [23] and path planning in robotics [2] to name a few.

Low-discrepancy point sets and sequences have typically been constructed using number theoretic properties [9, 16, 24, 29] where consequently the best results are obtained for special values of n such as powers of 2 or large prime numbers, and there has been a strong emphasis on asymptotic convergence rates as $n \rightarrow \infty$. Recently, there has been a growing interest in using computationally intense optimization methods to obtain low discrepancy points [6, 7, 28] and, contrary to the above, these methods are not asymptotic but rather optimize for some specific value of n and d .

Given the multitude of discrepancy criteria [3], these new methods raise the question of which one should be the target of the optimization. The L_∞ star discrepancy is perhaps the most widely studied, largely due to its connection in the Koksma–Hlawka inequality [15, 27] which bounds the integration error in terms of the variation of the integrand and the discrepancy of the point set. However, it is extremely difficult to compute in practice as it requires consideration of $O(n^d)$ rectangular regions and the best exact algorithm for it [10] costs $O(n^{d/2+1})$. In addition to its high cost, it is not differentiable with respect to the input points, which makes it impossible to optimize via gradient-based methods.

A traditional way to circumvent this issue has been to study the L_2 star discrepancy, denoted D_2^* . Unlike the L_∞ star discrepancy, there exists a closed-form expression for the L_2 star discrepancy, called the Warnock formula [33]:

$$(D_2^*(\{\mathbf{x}_i\}_{i=1}^n))^2 := \frac{1}{3^d} - \frac{2}{n} \sum_{i=1}^n \prod_{j=1}^d \frac{1 - x_{ij}^2}{2} + \frac{1}{n^2} \sum_{i,i'=1}^n \prod_{j=1}^d 1 - \max(x_{ij}, x_{i'j})$$

for an n -element point set $\{\mathbf{x}_1, \dots, \mathbf{x}_n\}$ contained in $[0, 1]^d$ where $x_{ij} \in [0, 1]$ denotes the j^{th} component of \mathbf{x}_i for all $1 \leq i \leq n$ and $1 \leq j \leq d$. Not only can this clearly be computed in $O(dn^2)$ time, it is a continuous function of the input points, and is differentiable almost everywhere. Furthermore, it is not devoid of theoretical properties, as there exist L_2 analogues of the Koksma–Hlawka inequality [12, 21].

Both of these star discrepancies are defined through anchored boxes, that is, hyper-rectangular subsets of $[0, 1]^d$ which include the origin. Emphasizing the origin over the other $2^d - 1$ vertices in $\{0, 1\}^d$ simplifies the analysis of such point sets, but is not always well suited to a given integration problem. Indeed, as each parameter range is typically rescaled to $[0, 1]$, anchoring at the origin implicitly suggests that minimal parameter values are more important, an assumption which rarely applies. This asymmetry was famously observed by Matoušek in [22] and we will refer to it here as *Pathology I*, although similar concerns appear to have arisen earlier or independently in the literature, e.g., in work by Hickernell around the same time [12]. Another serious issue arises in the form of *Pathology II*, also observed by Matoušek in [22], who shows that placing

all n points at $\mathbf{1} = (1, 1, \dots, 1)$ can yield a smaller L_2 star discrepancy than the expected value for n IID uniform points—despite the latter being clearly more evenly distributed. This pathology persists until n becomes exponentially large in the dimension. These observations motivate this work for further study, both theoretically and computationally, on the optimization of discrepancy measures.

1.1 Contributions

Tackling these two key issues leads us to introduce the *average squared discrepancy*, denoted by D_2^{asd} . This measure consists of averaging 2^d versions of the L_2 star discrepancy, one for each corner of $[0, 1]^d$. While this nominally raises the computational cost by a factor of 2^d with a naive computation method, we show that there is a ‘Warnock formula’ for it at cost $O(dn^2)$ in Theorem 1. We point out that this measure corresponds to the L_2 analog of the *multiple-corner* discrepancy recently introduced in [6]. Furthermore, by using the associated Warnock formula, we show that the average squared discrepancy is, by a constant factor, equivalent to a weighted symmetric discrepancy with judiciously chosen weights introduced by Hickernell in [12] using a reproducing kernel Hilbert space (RKHS) approach, providing a much simpler motivation for that RKHS criterion.

To tackle the second problem highlighted by Matoušek, we consider a wide range of traditional discrepancy measures known to avoid giving special treatment to the origin. We show that, surprisingly, only the average squared discrepancy circumvents this pathology as summarized in Proposition 3 and Table 1.

Our final contribution is a numerical comparison of the different discrepancy measures introduced in dimension $d = 2$ (higher dimensions would require to weigh the dimensions, which is beyond the scope of this paper). For this, we first use the Message-Passing Monte Carlo framework [28] to obtain optimized points sets for each discrepancy criterion. These optimized sets are compared on two different levels. First, we compare them to the traditional Sobol’ points, regularly used by practitioners who require well-distributed point sets, and show that our sets have a 10 to 40% lower discrepancy depending on the criteria. Secondly, using these sets optimized for different criteria, we compare their values for the L_2 star discrepancy. We show that the average squared discrepancy optimized sets lead to barely higher values for the L_2 star discrepancy than the star discrepancy optimization itself.

1.2 Paper Overview

An outline of this paper is as follows. Section 2 describes classical discrepancy measures, starting with the star discrepancies and then moves to consider measures which do not give special consideration to the origin of $[0, 1]^d$. It also lists a number of formulas to compute these discrepancies, currently spread out in the literature, in Section 2.3 as well as a formula for a new centered discrepancy in Section 2.4. A reader familiar with the literature may begin reading there without losing out. Section 3 introduces the average squared discrepancy, and

shows that it is the only one that does not present the issue highlighted by Matoušek. Section 4 presents numerical results comparing the optimization of the different discrepancy measures. Finally, Section 4.2 presents a greedy sequential construction approach, inspired by Kritzinger’s [20] construction for the L_2 star discrepancy in one dimension.

2 Classical discrepancies

For integers $n, d \geq 1$, we study the discrepancy of the points $\mathbf{x}_1, \dots, \mathbf{x}_n \in [0, 1]^d$. Given a measurable set $A \subset [0, 1]^d$, the local discrepancy of A is

$$\delta(A) = \delta(A; \mathbf{x}_1, \dots, \mathbf{x}_n) = \frac{1}{n} \sum_{i=1}^n 1\{\mathbf{x}_i \in A\} - |A|$$

where $|\cdot|$ is the usual Lebesgue measure.

2.1 Star discrepancies

In the early 20th century, research primarily focused on the uniform placement of points in $[0, 1]^d$ with respect to unanchored axis-parallel boxes. The Weyl criterion for equidistribution [34, 35] is a prominent example of this. While it is difficult to pinpoint the exact point in the literature, a shift occurred around the mid-20th century towards a discrepancy which considered axis-parallel boxes anchored at the origin—which was later referred to as the *star discrepancy*. This shift in focus was likely motivated by practical considerations; the star discrepancy is both computationally and conceptually simpler than the extreme discrepancy while maintaining the same asymptotic behavior in n .

Definition 2.1 (L_∞ star discrepancy). *The L_∞ star discrepancy is*

$$D_\infty^* = D_\infty^*(\mathbf{x}_1, \dots, \mathbf{x}_n) = \sup_{\mathbf{a} \in [0, 1]^d} |\delta([\mathbf{0}, \mathbf{a}])| \quad (1)$$

where $[\mathbf{0}, \mathbf{a}] = \{\mathbf{x} \in [0, 1]^d \mid 0 \leq x_j < a_j, 1 \leq j \leq d\}$ is the anchored box at \mathbf{a} .

In other words, it corresponds to the greatest absolute difference between the volume of a box anchored at the origin and the proportion of points that falls inside this box. As noted in the introduction, while of theoretical importance, this quantity is not well suited to numerical optimization and is usually replaced by its L_2 variant.

Definition 2.2 (L_2 star discrepancy). *The L_2 star discrepancy is defined by*

$$D_2^* = D_2^*(\mathbf{x}_1, \dots, \mathbf{x}_n) = \left(\int_{[0, 1]^d} \delta([\mathbf{0}, \mathbf{a}])^2 d\mathbf{a} \right)^{1/2}. \quad (2)$$

It can be seen as the average local discrepancy over $[0, 1]^d$. Its computation in dimension 1 can be traced back to [36], while Warnock’s formula [33], given below, is the tool to be used in any dimension.

$$(D_2^*)^2 = \frac{1}{3^d} - \frac{2}{n} \sum_{i=1}^n \prod_{j=1}^d \frac{1 - x_{ij}^2}{2} + \frac{1}{n^2} \sum_{i,i'=1}^n \prod_{j=1}^d [1 - \max(x_{ij}, x_{i'j})]. \quad (3)$$

Importantly, it is continuous in x_{ij} and it can be computed in $O(dn^2)$ time, making it much more practical than the L_∞ equivalent. While Heinrich [11] shows how to compute it in $O(n(\log n)^d)$ time—a better algorithm for small dimensions—the simplicity of equation (3) makes it the usual choice.

For large d , most anchored boxes have a very small volume. Then placing a point \mathbf{x}_i near the origin creates a large discrepancy, as it will be counted for all these small boxes. This issue underlies Matoušek’s criticism (Pathology I) and is why the criterion is smaller when $\mathbf{x}_1 = \dots = \mathbf{x}_n = \mathbf{1}$ than its root mean square value under $\mathbf{x}_i \stackrel{\text{iid}}{\sim} \mathcal{U}[0, 1]^d$ when $n < (3/2)^d - 1$ [22].

2.2 Moving away from origin-anchored boxes

To remove the specific status of the origin, the usual solution is to consider a larger set of boxes, not limited to boxes anchored in the origin. We take a geometric approach when defining general L_2 discrepancies, i.e., each family of test sets A admits a well-defined geometric interpretation. For notational convenience downstream, we define all discrepancy notions in their squared form. Many of our discrepancy measures are defined in terms of rectangular hulls. For $a, b \in [0, 1]$ we let $\text{rect}(a, b) = [\min(a, b), \max(a, b)]$. Then the rectangular hull of $\mathbf{a}, \mathbf{b} \in [0, 1]^d$ is

$$\text{rect}(\mathbf{a}, \mathbf{b}) = \prod_{j=1}^d \text{rect}(a_j, b_j).$$

We will also denote the nearest vertex to $\mathbf{a} \in [0, 1]^d$ by $\mathbf{v}(\mathbf{a})$. Defining

$$v_j(\mathbf{a}) = \mathbf{1}_{\{a_j \geq 1/2\}}$$

ensures uniqueness when $a_j = 1/2$ for some $j = 1, \dots, d$.

None of the measures we consider depend on whether the rectangles we use are open or closed or half-open because we are averaging over the locations of their boundary points. When using methods from the literature we may change the open-ness or closed-ness from the way those methods were originally presented in order to get a simpler presentation here.

Definition 2.3 (Extreme discrepancy). *The L_∞ discrepancy taking over all axis-aligned boxes $[\mathbf{a}, \mathbf{b}] \subset [0, 1]^d$ is called the extreme discrepancy. The analogous (squared) L_2 extreme discrepancy is*

$$(D_2^{\text{ext}})^2 = \int_{[0,1]^d} \int_{[0,1]^d} \mathbf{1}_{\{\mathbf{a} \leq \mathbf{b}\}} \delta([\mathbf{a}, \mathbf{b}])^2 d\mathbf{a} d\mathbf{b}, \quad (4)$$

where $\mathbf{a} \leq \mathbf{b}$ holds component-wise.

Motivated by integration of periodic functions, [12] defines the *periodic* or *wraparound discrepancy*, which treats $[0, 1)^d$ as a torus. For $a, b \in [0, 1]$, define

$$W(a, b) = \begin{cases} [a, b), & a \leq b, \\ [0, b) \cup [a, 1), & a > b, \end{cases}$$

and extend to $\mathbf{a}, \mathbf{b} \in [0, 1]^d$ by

$$W(\mathbf{a}, \mathbf{b}) = \prod_{j=1}^d W(a_j, b_j).$$

Definition 2.4 (Periodic discrepancy). *The L_2 periodic discrepancy is defined as*

$$(D_2^{\text{per}})^2 = \int_{[0,1]^d} \int_{[0,1]^d} \delta(W(\mathbf{a}, \mathbf{b}))^2 d\mathbf{a} d\mathbf{b}. \quad (5)$$

Note that all the boxes used for the star discrepancy are contained in the set of boxes used for the extreme discrepancy, itself contained in the set of boxes for the periodic discrepancy. Hickernell [12] introduced the *centered discrepancy*, where the test boxes are the set of axis-aligned boxes connecting a point $\mathbf{a} \in [0, 1]^d$ to the closest vertex of the cube.

Definition 2.5 (Centered discrepancy). *The L_2 centered discrepancy is*

$$(D_2^{\text{ctr}})^2 = \int_{[0,1]^d} \delta(\text{rect}(\mathbf{a}, \mathbf{v}(\mathbf{a})))^2 d\mathbf{a}. \quad (6)$$

A related construction leads to the *symmetric discrepancy*, which uses unions of boxes defined by all even vertices of the hypercube. Given $\mathbf{a} \in [0, 1]^d$ and a vertex $\mathbf{v} \in \{0, 1\}^d$, $\text{rect}(\mathbf{a}, \mathbf{v}(\mathbf{a}))$ defines an orthant for \mathbf{a} anchored at the vertex $\mathbf{v}(\mathbf{a})$. Let $E = \{\mathbf{v} \in \{0, 1\}^d \mid \sum_{j=1}^d v_j \text{ is even}\}$. The union of the “even” orthants is

$$\text{orth}_e(\mathbf{a}) = \bigcup_{\mathbf{v} \in E} \text{rect}(\mathbf{a}, \mathbf{v}).$$

Definition 2.6 (Symmetric discrepancy). *The L_2 symmetric discrepancy is*

$$(D_2^{\text{sym}})^2 = \int_{[0,1]^d} \delta(\text{orth}_e(\mathbf{a}))^2 d\mathbf{a}. \quad (7)$$

The centered and symmetric discrepancies introduced by Hickernell [12] are originally presented in a more general form that includes projections onto lower-dimensional faces. We focus here on their purely d -dimensional formulations.

Another discrepancy may be defined by anchoring each test box at the center $\mathbf{c} = (1/2, \dots, 1/2)$ of the cube, leading to the *centered-anchor discrepancy*.

Definition 2.7 (Centered-anchor discrepancy). *The L_2 centered-anchor discrepancy is given by*

$$(D_2^{\text{cad}})^2 = \int_{[0,1]^d} \delta(\text{rect}(\mathbf{a}, \mathbf{c}))^2 d\mathbf{a}.$$

A Warnock-type formula for this criterion is derived in Section 2.4, though due to discontinuities when $x_{ij} = 1/2$, it is not suitable for optimization and it was not included in our computations.

Finally, we mention the L_2 mixture discrepancy, introduced by Zhou, Fang, and Ning [37], which combines elements of the centered and periodic discrepancies. Although it is not easily expressed in terms of subsets $A \subset [0, 1]^d$, we include it here to provide, to the best of the authors' knowledge, a complete survey of known L_2 discrepancy measures.

2.3 Computing the L_2 discrepancies, known formulas

We already highlighted that the L_2 star discrepancy can be computed efficiently using the Warnock formula. Despite these other discrepancies being characterized by a larger set of boxes, they are all known to present a similar formula, which can also be computed in $O(dn^2)$ time. While these expressions were all previously known, they are scattered across various sources. In this section, we present a consolidated survey of such expressions.

One distinction between discrepancy measures is the way that they treat marginal effects, by which we mean the discrepancy of coordinate projections of the points. The geometric discrepancy measures we have presented prior to this point describe fully d -dimensional subsets of $[0, 1]^d$. Marginal sets, such as boxes with some sides of length 1, have measure zero in our L_2 formulas.

We will present firstly measures just ignoring the marginal effects, and will later establish the link to those that incorporate lower-dimensional projections in Section 2.5. We do this to be consistent with how we have defined the measures in Section 2.2 and only these measures are implemented in our numerical experiments in Section 4. In any case where a measure has been adapted from its original source, this is stated explicitly.

To begin, Hinrichs, Kritzing and Pillichshammer [1, Proposition 13] show that

$$\begin{aligned} (D_2^{\text{ext}})^2 = & \frac{1}{12^d} - \frac{2}{n} \sum_{i=1}^n \prod_{j=1}^d \frac{x_{ij}(1-x_{ij})}{2} \\ & + \frac{1}{n^2} \sum_{i,i'=1}^n \prod_{j=1}^d (\min(x_{ij}, x_{i'j}) - x_{ij}x_{i'j}) \quad (8) \end{aligned}$$

after adjusting from count discrepancies to volume discrepancies. They credit [33] for this formula. For $n = 1$, $(D_2^{\text{ext}})^2 = 12^{-d} + (1 - 2^{-d+1}) \prod_{j=1}^d x_{1j}(1-x_{1j})$

and when $d = 1$, any placement of $x_1 \in [0, 1]$ attains $D_2^{\text{ext}} = 1/\sqrt{12}$. For $n = 1$ and $d \geq 2$, the best choice for \mathbf{x}_1 is either $\mathbf{0}$ or $\mathbf{1}$.

The same authors also provide a formula for the L_2 periodic discrepancy, which is

$$(D_2^{\text{per}})^2 = -\frac{1}{3^d} + \frac{1}{n^2} \sum_{i,i'=1}^n \prod_{j=1}^d \left(\frac{1}{2} - |x_{ij} - x_{i'j}| + (x_{ij} - x_{i'j})^2 \right) \quad (9)$$

again adjusting from count discrepancies. They cite Hinrichs and Oettershagen [14] for it as well as Novak and Wozniakowski [25].

Formulas for the L_2 symmetric and centered discrepancies appear in [12] where they are presented in a more general setting incorporating the marginal effects. For now, maintaining consistency with (6) and (7), we present

$$\begin{aligned} (D_2^{\text{ctr}})^2 &= \frac{1}{12^d} - \frac{2}{n} \sum_{i=1}^n \prod_{j=1}^d \frac{1}{2} (|x_{ij} - 1/2| - (x_{ij} - 1/2)^2) \\ &\quad + \frac{1}{n^2} \sum_{i,i'=1}^n \prod_{j=1}^d \frac{1}{2} (|x_{ij} - 1/2| + |x_{i'j} - 1/2| - |x_{ij} - x_{i'j}|) \end{aligned} \quad (10)$$

and

$$(D_2^{\text{sym}})^2 = \frac{1}{12^d} - \frac{2}{n} \sum_{i=1}^n \prod_{j=1}^d \frac{x_{ij}(1-x_{ij})}{2} + \frac{1}{n^2} \sum_{i,i'=1}^n \prod_{j=1}^d \frac{1-2|x_{ij}-x_{i'j}|}{4}. \quad (11)$$

Finally, the L_2 mixture discrepancy adapted from [37] to consider only the d -dimensional distribution is given as

$$\begin{aligned} (D_2^{\text{mix}})^2 &= \left(\frac{7}{12} \right)^d - \frac{2}{n} \sum_{i=1}^n \prod_{j=1}^d \left(\frac{2}{3} - \frac{1}{4}|x_{ij} - 1/2| - \frac{1}{4}(x_{ij} - 1/2)^2 \right) \\ &\quad + \frac{1}{n^2} \sum_{i,i'=1}^n \prod_{j=1}^d \left(\frac{7}{8} - \frac{1}{4}|x_{ij} - 1/2| - \frac{1}{4}|x_{i'j} - 1/2| - \frac{3}{4}|x_{ij} - x_{i'j}| + \frac{1}{2}|x_{ij} - x_{i'j}|^2 \right). \end{aligned}$$

2.4 Formula for the L_2 center-anchored discrepancy

The centered-anchor discrepancy, D_2^{cad} , introduced above in Definition 2.7, uses $\mathbf{c} = (1/2, \dots, 1/2)$ as the anchor for test boxes; an intuitively better choice than favoring the origin as the anchor as per the star discrepancy. We now develop a Warnock-type $O(dn^2)$ computation for this measure. Notably, this measure is discontinuous at $\mathbf{x}_i = \mathbf{c}$, making it unsuitable for optimization, however, we include it in our study to provide a comprehensive review of L_2 measures that treat all corners of the unit hypercube symmetrically.

Proposition 1. *In the above notation*

$$(D_2^{\text{cad}})^2 = \frac{1}{12^d} - \frac{2}{n} \sum_{i=1}^n \prod_{j=1}^d \frac{x_{ij}(1-x_{ij})}{2} + \frac{1}{n^2} \sum_{i,i'=1}^n \mathbf{1}_{\{\mathbf{v}(\mathbf{x}_i)=\mathbf{v}(\mathbf{x}_{i'})\}} \prod_{j=1}^d \min(|x_{ij} - v(x_{ij})|, |x_{i'j} - v(x_{i'j})|). \quad (12)$$

Proof. For any $\mathbf{x} \in [0, 1]^d$ and almost all $\mathbf{a} \in [0, 1]^d$, $\mathbf{x} \in \text{rect}(\mathbf{a}, \mathbf{c})$ means that for each j , either $c_j < x_j < a_j < 1$ or $c_j > x_j > a_j > 0$. Therefore, we will work as if $\mathbf{x} \in \text{rect}(\mathbf{a}, \mathbf{c})$ is equivalent to $\mathbf{a} \in \text{rect}(\mathbf{x}, \mathbf{v}(\mathbf{x}))$, where we recall that $\mathbf{v}(\mathbf{x})$ is the vertex of $\{0, 1\}^d$ closest to \mathbf{x} . Any differences arising from equalities among c_j , x_j and a_j will not affect our integrals and neither will the distinction between open or closed boundaries of our rectangles.

Next

$$\begin{aligned} \int_{[0,1]^d} \delta(\text{rect}(\mathbf{a}, \mathbf{c}))^2 d\mathbf{a} &= \int_{[0,1]^d} \left(\prod_{j=1}^d |a_j - 1/2| - \frac{1}{n} \sum_{i=1}^n \mathbf{1}_{\{\mathbf{x}_i \in \text{rect}(\mathbf{a}, \mathbf{c})\}} \right)^2 d\mathbf{a} \\ &= \frac{1}{12^d} - \frac{2}{n} \sum_{i=1}^n \int_{\text{rect}(\mathbf{x}_i, \mathbf{v}(\mathbf{x}_i))} \prod_{j=1}^d |a_j - 1/2| d\mathbf{a} \\ &\quad + \frac{1}{n^2} \sum_{i,i'=1}^n \text{vol}(\text{rect}(\mathbf{x}_i, \mathbf{v}(\mathbf{x}_i)) \cap \text{rect}(\mathbf{x}_{i'}, \mathbf{v}(\mathbf{x}_{i'}))). \end{aligned}$$

If $x_{ij} > 1/2$, then $\mathbf{v}(\mathbf{x}_i)_j = 1$ and

$$\int_{\text{rect}(\mathbf{x}_{ij}, \mathbf{v}(\mathbf{x}_i)_j)} |a_j - 1/2| da_j = \int_{x_{ij}}^1 (a_j - 1/2) da_j = \frac{1}{2}(x_{ij} - x_{ij}^2).$$

If $x_{ij} < 1/2$, then $\mathbf{v}(\mathbf{x}_i)_j = 0$ and

$$\int_{\text{rect}(\mathbf{x}_{ij}, \mathbf{v}(\mathbf{x}_i)_j)} |a_j - 1/2| da_j = \int_0^{x_{ij}} (1/2 - a_j) da_j = \frac{1}{2}(x_{ij} - x_{ij}^2)$$

as well. Next,

$$\begin{aligned} &\text{vol}(\text{rect}(\mathbf{x}_i, \mathbf{v}(\mathbf{x}_i)) \cap \text{rect}(\mathbf{x}_{i'}, \mathbf{v}(\mathbf{x}_{i'}))) \\ &= \mathbf{1}_{\{\mathbf{v}(\mathbf{x}_i)=\mathbf{v}(\mathbf{x}_{i'})\}} \prod_{j=1}^d \min(|x_{ij} - v(x_{ij})|, |x_{i'j} - v(x_{i'j})|) \end{aligned}$$

where $v(\cdot)$ is the vertex finding function on $[0, 1]$. Finally, $\int_{[0,1]^d} \delta(\text{rect}(\mathbf{a}, \mathbf{c}))^2 d\mathbf{a}$ equals

$$\begin{aligned} & \frac{1}{12^d} - \frac{2}{n} \sum_{i=1}^n \prod_{j=1}^d \frac{x_{ij}(1-x_{ij})}{2} \\ & + \frac{1}{n^2} \sum_{i,i'=1}^n \mathbf{1}_{\{\mathbf{v}(\mathbf{x}_i)=\mathbf{v}(\mathbf{x}_{i'})\}} \prod_{j=1}^d \min(|x_{ij} - v(x_{ij})|, |x_{i'j} - v(x_{i'j})|). \end{aligned}$$

□

2.5 Discrepancies involving marginal effects

Hickernell was among the first to formalize the connection between discrepancy theory and reproducing kernel Hilbert spaces (RKHS); see [12] and references therein. Although we do not detail this approach here, it is important to note that Hickernell's framework defines discrepancies via ANOVA-type decompositions, and therefore inherently includes marginal effects. That is, contributions from projections of the point set onto lower-dimensional subsets of coordinates.

Fortunately, the relationship between discrepancies that consider only full-dimensional effects and those incorporating marginal contributions can be understood in terms of the symmetric and positive definite kernels associated with the RKHS. Specifically, if $\prod_{j=1}^d \tilde{K}(x_j, y_j)$ denotes the product kernel corresponding to a discrepancy that evaluates only the full d -dimensional distribution (excluding projections), then the analogous kernel incorporating all marginal effects is given by: $K(\mathbf{x}, \mathbf{y}) = \prod_{j=1}^d \left(1 + \gamma_j \tilde{K}(x_j, y_j)\right)$ where $\boldsymbol{\gamma} = (\gamma_1, \dots, \gamma_d)$ is a vector of non-negative weights following the framework of [30]. This kernel gives rise to weighted variants of standard L_2 discrepancy measures.

For example, the weighted L_2 centered and symmetric discrepancies take the forms:

$$\begin{aligned} (D_2^{\text{ctr}, \boldsymbol{\gamma}})^2 &= \prod_{j=1}^d \left(1 + \frac{\gamma_j}{12}\right) - \frac{2}{n} \sum_{i=1}^n \prod_{j=1}^d \left[1 + \frac{\gamma_j}{2} \left(\left|x_{ij} - \frac{1}{2}\right| - \left|x_{ij} - \frac{1}{2}\right|^2\right)\right] \\ &+ \frac{1}{n^2} \sum_{i,i'=1}^n \prod_{j=1}^d \left[1 + \frac{\gamma_j}{2} \left(\left|x_{ij} - \frac{1}{2}\right| + \left|x_{i'j} - \frac{1}{2}\right| - |x_{ij} - x_{i'j}|\right)\right] \quad (13) \end{aligned}$$

and

$$\begin{aligned} (D_2^{\text{sym}, \boldsymbol{\gamma}})^2 &= \prod_{j=1}^d \left(1 + \frac{\gamma_j}{12}\right) - \frac{2}{n} \sum_{i=1}^n \prod_{j=1}^d \left(1 + \frac{\gamma_j}{2} x_{ij}(1-x_{ij})\right) \\ &+ \frac{1}{n^2} \sum_{i,i'=1}^n \prod_{j=1}^d \left[1 + \frac{\gamma_j}{4} (1 - 2|x_{ij} - x_{i'j}|)\right]. \quad (14) \end{aligned}$$

Similar weighted variants exist for all L_2 discrepancy measures presented in Section 2.2.

Remark 1. Setting $\gamma = \mathbf{1} = (1, \dots, 1)$ in (13) and $\gamma = \mathbf{4} = (4, \dots, 4)$ in (14) recovers the forms of the centered and symmetric discrepancies originally presented in [12].

3 The average squared discrepancy

Another way of eliminating the special status of the origin is by treating each vertex of $[0, 1]^d$ in turn as the origin and averaging. As mentioned previously, this was first done analogously for the L_∞ star discrepancy in [6], where it is called 'multiple-corner' discrepancy. For $u \subseteq \{1, 2, \dots, d\}$ and $i = 1, \dots, n$, let

$$x_{ij}^u = \begin{cases} x_{ij}, & j \in u \\ 1 - x_{ij}, & \text{else} \end{cases}$$

be a partial reflection of the point \mathbf{x}_i .

Definition 3.1 (Average squared discrepancy). *The L_2 average squared discrepancy is defined as*

$$(D_2^{\text{asd}})^2 = \frac{1}{2^d} \sum_{u \subseteq 1:d} D_2^*(\mathbf{x}_1^u, \dots, \mathbf{x}_n^u)^2. \quad (15)$$

By linearity of expectation, $\mathbb{E}((D_d^{\text{asd}})^2) = \mathbb{E}((D_2^*)^2) = (2^{-d} - 3^{-d})/n$ for $\mathbf{x}_i \stackrel{\text{iid}}{\sim} U[0, 1]^d$.

Although (15) involves a summation over 2^d terms, it can be computed with the same computational complexity as the other L_2 discrepancies considered thus far. The next theorem gives a Warnock formula for it.

Theorem 1. *In the above notation*

$$(D_2^{\text{asd}})^2 = \frac{1}{3^d} - \frac{2}{n} \sum_{i=1}^n \prod_{j=1}^d \frac{1 + 2x_{ij} - 2x_{ij}^2}{4} + \frac{1}{n^2} \sum_{i,i'=1}^n \prod_{j=1}^d \frac{1 - |x_{ij} - x_{i'j}|}{2}. \quad (16)$$

Proof. Plugging the Warnock formula (3) into the definition (15) shows that $(D_2^{\text{asd}})^2$ equals

$$\frac{1}{3^d} - \frac{2}{n} \sum_{i=1}^n \sum_{u \subseteq 1:d} \prod_{j=1}^d \frac{1 - (x_{ij}^u)^2}{4} + \frac{1}{n^2} \sum_{i,i'=1}^n \sum_{u \subseteq 1:d} \prod_{j=1}^d \frac{\min(1 - x_{ij}^u, 1 - x_{i'j}^u)}{2}.$$

Now

$$\sum_{u \subseteq 1:d} \prod_{j=1}^d \frac{1 - (x_{ij}^u)^2}{4} = \prod_{j=1}^d \frac{1 - x_{ij}^2 + 1 - (1 - x_{ij})^2}{4} = \prod_{j=1}^d \frac{1 + 2x_{ij} - 2x_{ij}^2}{4}$$

and then

$$\begin{aligned}
& \sum_{u \subseteq [1:d]} \prod_{j=1}^d \frac{\min(1 - x_{ij}^u, 1 - x_{i'j}^u)}{2} \\
&= \prod_{j=1}^d \frac{\min(1 - x_{ij}, 1 - x_{i'j}) + \min(1 - (1 - x_{ij}), 1 - (1 - x_{i'j}))}{2} \\
&= \prod_{j=1}^d \frac{1 + \min(x_{ij}, x_{i'j}) - \max(x_{ij}, x_{i'j})}{2}
\end{aligned}$$

from which the result follows. \square

We observe the following unexpected equivalence between the average squared discrepancy and Hickernell's symmetric discrepancy from [12], despite the differences in how these measures are constructed.

Proposition 2. *In the above notation,*

$$4^d (D_2^{\text{asd}})^2 = (D_2^{\text{sym}, \gamma})^2,$$

where $\gamma = \mathbf{4} = (4, \dots, 4)$.

Proof. This identity follows by direct comparison of equations (14) and (16). \square

3.1 Matoušek's Criticism

Referred to as Pathology II in the Introduction, Matoušek observed that the L_2 star discrepancy, D_2^* , assigns a smaller value to n identical copies of the point $\mathbf{1} = (1, \dots, 1)$ than the expected value for n IID points from $[0, 1]^d$, unless n is exponentially large in d [22]. This behavior is clearly undesirable since discrepancy measures, among other things, are intended to capture point set uniformity.

One might hope that this issue arises solely because D_2^* privileges the origin, and that many of the other measures considered in Section 2.2 avoid this problem. However, this turns out not to be the case. Indeed, many other L_2 discrepancies—despite being constructed to treat all vertices of $[0, 1]^d$ symmetrically—still exhibit the same issue: placing all n points at a single “special” location (e.g., the center or a cube vertex) can lead to lower discrepancy than n IID points.

All the discrepancies we consider share the same general structure:

$$A - \frac{2}{n} \sum_{i=1}^n \prod_{j=1}^d B(x_{ij}) + \frac{1}{n^2} \sum_{i, i'=1}^n \prod_{j=1}^d C(x_{ij}, x_{i'j}),$$

for constants A and functions B, C specific to the discrepancy. Then for $\mathbf{x}_i \sim_{\text{iid}} U[0, 1]^d$, the expectation simplifies to

$$A - 2\mathbb{E}[B(u)]^d + \left(1 - \frac{1}{n}\right) \mathbb{E}[C(u, v)]^d + \frac{1}{n} \mathbb{E}[C(u, u)]^d, \quad (17)$$

Method	$n\mathbb{E}((D_2^\bullet)^2)$	Single point	$D_2^2(\text{single point})$	$n >$
*	$2^{-d} - 3^{-d}$	$(1, \dots, 1)$	3^{-d}	$(3/2)^d - 1$
ext	$6^{-d} - 12^{-d}$	any vertex	12^{-d}	$2^d - 1$
per	$2^{-d} - 3^{-d}$	any point	3^{-d}	$(3/2)^d - 1$
ctr	$4^{-d} - 12^{-d}$	center \mathbf{c}	12^{-d}	$3^d - 1$
cad	$2^{-d} - 12^{-d}$	center \mathbf{c}	$12^{-d} - 2 \cdot 8^{-d} + 2^{-d}$	$6^d - 1$
mix	$(3/4)^d - (7/12)^d$	any vertex	see text	$\approx (9/7)^d$
sym	$4^{-d} - 12^{-d}$	center \mathbf{c}	$12^{-d} - 2 \cdot 8^{-d} + 4^{-d}$	1
asd	$2^{-d} - 3^{-d}$	center \mathbf{c}	$2^{-d} - 2(3/8)^d + 3^{-d}$	1

Table 1: Summary of expected squared L_2 discrepancies for IID points, the repeated single point minimizers and their discrepancy, and the threshold n at which IID sampling outperforms repeated placement.

with $u, v \sim U[0, 1]$ independently.

As an example, for D_2^{ext} , we find $\mathbb{E}[D_2^{\text{ext}}]^2 = \frac{1}{n}(6^{-d} - 12^{-d})$, but $(D_2^{\text{ext}})^2 = 12^{-d}$ when n points are placed identically at any vertex. Hence, IID sampling only becomes better when $n > 2^d - 1$, and hence, in this sense, the L_2 extreme discrepancy is even worse than the star equivalent which only requires $n > (3/2)^d - 1$ points. Moreover, this behavior is not unique to D_2^{ext} . Almost all of the classical discrepancies exhibit a similar phenomenon: for small n , placing all points at a special location, either the center \mathbf{c} , a vertex, or an arbitrary point, yields lower discrepancy than using n IID samples. The only exceptions are D_2^{asd} (and thus its equivalent formulation $D_2^{\text{sym}, \gamma}$), and the unweighted symmetric discrepancy D_2^{sym} , which favor dispersed sampling even at small n .

These behaviors are summarized in Table 1, which records the expected discrepancy for IID points, the value at the optimal single point, and the threshold sample size n above which IID sampling is preferred. We finish this section highlighting the average squared discrepancy as a measure which does not suffer from Pathology II.

Proposition 3. *Let $\{\mathbf{x}_i\}_{i=1}^n \sim_{iid} U([0, 1]^d)$ and $\mathbf{c}_1 = \dots = \mathbf{c}_n = \mathbf{c}$, where $\mathbf{c} = (1/2, \dots, 1/2) \in [0, 1]^d$ is the center point. Then*

$$\mathbb{E} [D_2^{\text{asd}}(\mathbf{x}_1, \dots, \mathbf{x}_n)^2] < D_2^{\text{asd}}(\mathbf{c}_1, \dots, \mathbf{c}_n)^2$$

for all $n > 1$.

Proof. Omitted. Easy computation due to (17). \square

4 Numerical Results

We present a comprehensive numerical study employing recently introduced state-of-the-art sample point optimization techniques using a range of objective functions introduced above. Our analysis focuses on comparing resulting point

Measure / n	16	32	64	128	256
Star	44.6%	43.0%	41.4%	39.2%	32.5%
Symmetric	43.2%	34.6%	34.3%	31.4%	29.3%
Avg. Squared	35.1%	26.6%	24.7%	22.9%	23.5%
Extreme	34.4%	20.0%	21.9%	18.8%	27.9%
Center	32.4%	21.9%	22.8%	25.3%	19.1%
Periodic	26.2%	9.9%	12.9%	14.8%	21.8%
Mixture	19.4%	11.8%	9.6%	12.0%	9.9%

Table 2: Relative improvement of two-dimensional MPMC point sets trained via the discrepancy measure in the leftmost column over the discrepancy of the Sobol’ sequence evaluated on the same measure. Higher values indicate greater improvement relative to the baseline Sobol’.

sets in two-dimensions for n as powers of 2 using the Sobol’ sequence as a benchmark. As our optimization framework, we use the Message-Passing Monte Carlo method [28], a deep learning global optimization method, and a recently successful greedy approach from Kritzing [20] and extended by Clément [4].

4.1 Message-Passing Monte Carlo

Message-Passing Monte Carlo (MPMC) represents a significant advance in integrating QMC methods with modern machine learning. By leveraging geometric deep learning through graph neural networks, MPMC generates low-discrepancy point sets with respect to the uniform distribution on the d -dimensional unit hypercube. Importantly, in its original formulation, the training objective for MPMC is the L_2 star discrepancy (3). MPMC has later been extended to general distributions via a kernelized Stein discrepancy approach [19].

All experiments for MPMC have been run on NVIDIA DGX A100 GPUs. Each model was trained with Adam [18] with weight decay for at least 100k steps with training stopped once the learning rate reached a value less than 10^{-6} . MPMC hyperparameters were not tuned, but instead were chosen judiciously as follows: learning rate of 0.001, weight decay 10^{-6} , graph radius 0.35, 2 GNN layers and 32 hidden units each. For further model details, we refer the reader to [28].

As an initial experiment, we extend the MPMC framework to directly minimize $(D_2^\bullet)^2$ for $\bullet \in \{*, \text{ext}, \text{sym}, \text{ctr}, \text{per}, \text{asd}, \text{mix}\}$. We train two-dimensional point sets for $n = 2^m$ with $m = 4, 5, 6, 7, 8$. Table 2 presents the relative improvement of the trained sets over the Sobol’ sequence evaluated on the same measure. The exact discrepancy values are given in Appendix A as Table 3. Our results show that MPMC is effective at minimizing a wide range of L_2 discrepancy measures and consistently outperforms Sobol’ point sets when evaluated under the same criteria by 10 to 40%, with some discrepancies (i.e., star,

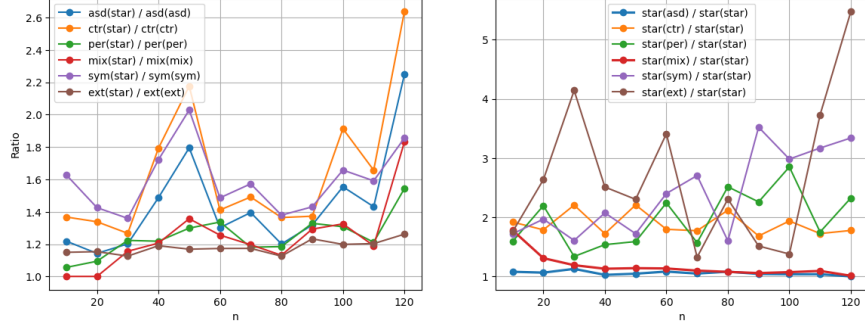


Figure 1: The left panel shows the ratio $(D_2^\bullet(\mathbf{x}_1, \dots, \mathbf{x}_n) / D_2^*(\tilde{\mathbf{x}}_1, \dots, \tilde{\mathbf{x}}_n))$, where $\mathbf{x}_1, \dots, \mathbf{x}_n \in [0, 1]^2$ are optimized for D_2^* and $\tilde{\mathbf{x}}_1, \dots, \tilde{\mathbf{x}}_n \in [0, 1]^2$ are optimized for D_2^\bullet , for each $\bullet \in \{\text{ext}, \text{per}, \text{sym}, \text{ctr}, \text{asd}, \text{mix}\}$. The right panel shows the ratio $(D_2^*(\tilde{\mathbf{x}}_1, \dots, \tilde{\mathbf{x}}_n) / D_2^\bullet(\mathbf{x}_1, \dots, \mathbf{x}_n))$, evaluating the star discrepancy on point sets optimized for each alternative criterion.

symmetric and average squared) benefiting more than others from optimization.

Figure 1 compares D_2^* with six alternative L_2 discrepancy measures, D_2^\bullet for $\bullet \in \{\text{ext}, \text{per}, \text{sym}, \text{ctr}, \text{asd}, \text{mix}\}$, under cross-evaluation: each panel shows the ratio between discrepancies evaluated on point sets optimized for one criterion and test on another. The left panel reveals that, especially as n increases, the D_2^* discrepancy of the star-optimal point set relative to the D_2^\bullet -optimal point set seems to grow steadily—demonstrating that point sets optimized for the asymmetric D_2^* criterion perform increasingly poorly when evaluated using alternative measures. This suggests that star-optimal points do not generalize well. Conversely, the right panel shows that point sets optimized for most alternative measures also yield poor D_2^* values—*except* for D_2^{mix} and D_2^{asd} , which produce near-optimal D_2^* values despite being optimized for different criteria. These two measures appear to induce well-balanced point sets that generalize well across discrepancy definitions. Full numerical results for this experiment appear in Appendix A, Table 4.

4.2 Greedy Approaches

We implement models for the direct optimization of low-discrepancy sequences with respect to the extreme, average squared, and centered L_2 discrepancies. While our experiments focus on these three criteria, the underlying framework is general and readily extends to any of the L_2 -based discrepancies discussed in this text. The approach is greedy: given an initial point set, each new point is selected to minimize the overall discrepancy when added. All experiments in this section were conducted using Gurobi, with a 120-second time limit imposed on each optimization instance. This approach is particularly relevant as practitioners frequently begin their experiments with a small budget (e.g. 20

points), and based on the results with this fixed budget decide to stop or add more points to sample from. It is then preferable to be able to re-use the already computed data, rather than having to start from a completely new point set.

Our construction is inspired by the strong empirical performance of the Kritzing sequence [20] for the L_2 star discrepancy. We adopt a similar sequential strategy, but generalize the objective to alternative L_2 discrepancies of interest.

Another advantage of L_2 -based discrepancy measures, not yet spoken about in this text, is that the contribution of a new point also admits a closed-form expression. For example, the contribution of a new point $y \in [0, 1]^d$ to the L_2 star discrepancy of points $\mathbf{x}_1, \dots, \mathbf{x}_n$ is given by

$$F(\mathbf{y}; \mathbf{x}_1, \dots, \mathbf{x}_n) := -2^{1-d} \prod_{j=1}^d (1 - y_j^2) + \frac{1}{n+1} \prod_{j=1}^d (1 - y_j) + \frac{2}{n+1} \sum_{i=1}^n \prod_{j=1}^d (1 - \max(y_j, x_{i,j})),$$

which can be evaluated in $\mathcal{O}(nd)$ time. This enables efficient greedy selection of the next point via

$$\mathbf{x}_{n+1} = \arg \min_{\mathbf{y} \in [0,1]^d} F(\mathbf{y}; \mathbf{x}_1, \dots, \mathbf{x}_n).$$

We extend this idea to other L_2 discrepancy variants, for which similar expressions for $F(\mathbf{y}; \mathbf{x}_1, \dots, \mathbf{x}_n)$ can often be derived. For further details, we refer the reader to [4, 5, 20].

Unlike the L_2 star discrepancy, the extreme, average squared, and centered L_2 discrepancies perform poorly when the sequence is initialized from a single-point set. In particular, for both the average squared and centered discrepancies, initializing at $(0.5, 0.5)$ leads to degenerate behavior: the optimal next point is repeatedly chosen as $(0.5, 0.5)$, resulting in a set containing only duplicated points.

To overcome this, we instead add multiple points at each step. While this approach alleviates the degeneracy, it comes with significantly higher computational cost. Figure 2 illustrates this strategy, showing the average squared and centered discrepancies when starting from the singleton set $\{(0.5, 0.5)\}$ and adding 4 points at a time—a natural choice given the symmetries in the definitions of these measures. The eventual rise in discrepancy values seen in Figure 2 is not due to a failure of the method, but rather a practical limitation: the optimizer reaches the 120-second time limit before it can identify a valid batch of 4 candidate points. This issue could be mitigated by relaxing the time constraint if needed.

Performance of the greedy selection algorithm improves noticeably when it is initialized from a high-quality point set—in this case, an MPMC point set optimized for the same discrepancy. Figure 3 (left) shows the evolution

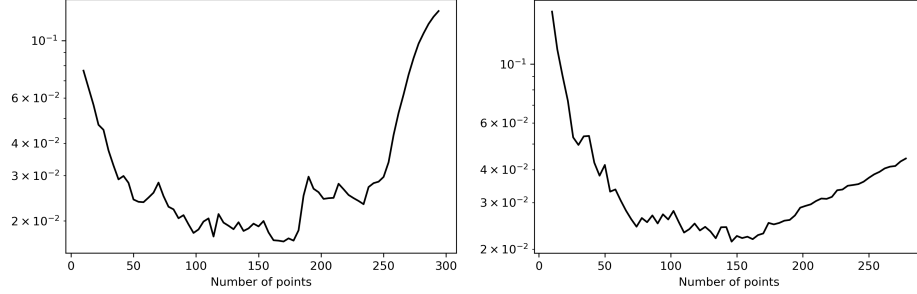


Figure 2: Average squared (left) and centered L_2 discrepancies (right) obtained when greedily adding 4 points at a time, starting with the singleton $\{(0.5, 0.5)\}$. The time limit is set at 120s for every 4 points to add, leading to the rise in discrepancy past a certain point.

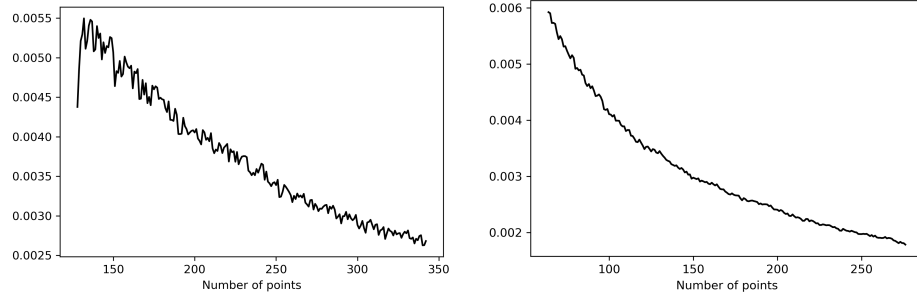


Figure 3: Average squared (left) and extreme (right) L_2 discrepancies obtained when greedily adding the single optimal point for the respective measures. Starting with MPMC set sizes of respectively 128 and 64 points.

of the average squared L_2 discrepancy as one point at a time is added to a $d = 2$, $n = 128$ MPMC set. While some improvement is observed, the final discrepancy remains higher than it could be largely due to a poor first step. Moreover, the resulting trajectory lacks the stability exhibited by the Kritzing sequence. In contrast, the L_2 extreme discrepancy shown in Figure 3 (right) displays behavior much closer to that of the Kritzing sequence—stable across iterations and consistently maintaining low discrepancy values.

5 Discussion

This paper provides a perspective on the “optimization-friendly” L_2 -based discrepancy measures, offering a comprehensive survey to support the design of

low-discrepancy point sets for QMC methods through direct optimization of L_2 -type measures. All measures discussed admit Warnock-type closed-form expressions, ensuring they remain computable in $O(n^2d)$ time, and are thus available for optimization workflows (except one, which was discontinuous, and thus unsuitable).

Of all the measures we considered, only the average squared discrepancy and the symmetric L_2 discrepancy (weighted and unweighted versions) avoid so-called Pathology II; repeated placement of n “special” points can yield a smaller discrepancy than n uniformly random IID points. We also noticed that the weighted symmetric L_2 discrepancy, that includes marginal contributions, is equivalent to the average squared discrepancy.

Our numerical results show that point set optimization through the discrepancy can be nontrivial in practice depending on the exact measure and the optimization method. We show that Message-Passing Monte Carlo, producing point sets with very small discrepancy, and greedy constructions, enabling sequential updating of excellent MPMC starting sets, offer robust methods consistently producing high-quality, very low-discrepancy point sets across discrepancy criteria.

Importantly, we find that optimizing the L_2 star discrepancy is not always advisable: it introduces an asymmetric origin bias that is exposed under symmetric evaluations, and is not recovered when alternative criteria are used to evaluate the resulting sets. In contrast, optimizing the symmetric average squared discrepancy yields good performance under the star discrepancy, suggesting that it promotes better generalization properties.

We hope this work encourages further interest in the optimization of discrepancy measures—both in the development of effective optimization methods and in the thoughtful selection of appropriate objective functions.

Acknowledgments. NK is supported by NSF grant DMS-2316011. ABO is supported by NSF grant DMS-2152780. We thank Fred J. Hickernell for several helpful conversations throughout the development of this manuscript. NK also acknowledges Lijia Lin and Ally Pascual Kwan for help running numerical experiments during their time as 2025 undergraduate summer research students at Illinois Tech supported by NSF Grant No. 2244553.

References

- [1] R. Kritzing, A. Hinrichs and F. Pillichshammer. Extreme and periodic L_2 discrepancy of plane point sets. *Acta Arithmetica*, 199:163–198, 2021.
- [2] M. Chahine, T K. Rusch, Z. J Patterson, and D. Rus. Improving efficiency of sampling-based motion planning via message-passing monte carlo. *arXiv preprint arXiv:2410.03909*, 2024.
- [3] W. Chen, A. Srivastav, and G. Travaglini, editors. *A Panorama of Discrepancy Theory*. Springer, Cham, Switzerland, 2014.

- [4] F. Clément. Extending the Kritzing sequence: more points and higher dimensions. <https://webia.lip6.fr/~fclement/fclement>, 2023.
- [5] F. Clément. *An Optimization Perspective on the Construction of Low-Discrepancy Point Sets*. PhD thesis, Sorbonne Université, 2024.
- [6] F. Clément, C. Doerr, K. Klamroth, and L. Paquete. Constructing optimal L_∞ star discrepancy sets, 2024.
- [7] F. Clément, C. Doerr, and L. Paquete. Star discrepancy subset selection: Problem formulation and efficient approaches for low dimensions. *J. Complexity*, 70:101645, 2022.
- [8] J. Dick, F. Kuo, and I. H. Sloan. High dimensional integration — the Quasi-Monte Carlo way. *Acta Numer.*, 22:133–288, 2013.
- [9] J. Dick and F. Pillichshammer. Discrepancy theory and quasi-Monte Carlo integration. In *A panorama of discrepancy theory*, pages 539–619. Springer, 2014.
- [10] D. P. Dobkin, D. Eppstein, and D. P. Mitchell. Computing the discrepancy with applications to supersampling patterns. *ACM Trans. Graph.*, 15:354–376, 1996.
- [11] S. Heinrich. Efficient algorithms for computing the l_2 -discrepancy. *Mathematics of Computation*, 65(216):1621–1633, 1996.
- [12] F. J. Hickernell. A generalized discrepancy and quadrature error bound. *Mathematics of Computation*, 67:299–322, 1998.
- [13] F. J. Hickernell, N. Kirk, and A. G. Sorokin. Quasi-Monte Carlo methods: What, Why, and How?, 2025.
- [14] A. Hinrichs and J. Oettershagen. Optimal point sets for quasi-Monte Carlo integration of bivariate periodic functions with bounded mixed derivatives. In *Monte Carlo and Quasi-Monte Carlo Methods*, pages 385–405, Cham, Switzerland, 2016. Springer.
- [15] E. Hlawka. Funktionen von beschränkter Variation in der Theorie der Gleichverteilung. *Annali di Matematica Pura ed Applicata*, 54:325–333, 1961.
- [16] F. Pillichshammer J. Dick, P. Kritzer. *Lattice Rules*. Springer, Cham, 2022.
- [17] A. Keller. Quasi-Monte Carlo radiosity. In *X. Pueyo and P. Schröder (Eds.), Eurographics Rendering Workshop*, pages 101–110, 1996.
- [18] D. P. Kingma and J. Ba. Adam: A method for stochastic optimization. *CoRR*, abs/1412.6980, 2014.

- [19] N. Kirk, T. K. Rusch, J. Zech, and D. Rus. Low stein discrepancy via Message-Passing Monte Carlo. *arXiv preprint arXiv:2503.21103*, 2025.
- [20] R. Kritzing. Uniformly distributed sequences generated by a greedy minimization of the l2 discrepancy. *Moscow Journal of Combinatorics and Number Theory*, 11(3):215–236, 2022.
- [21] L. Kuipers and H. Niederreiter. *Uniform Distribution of Sequences*. Wiley, New York, 1974.
- [22] J. Matoušek. *Geometric Discrepancy: An Illustrated Guide*. Springer-Verlag, Heidelberg, 1998.
- [23] S. Mishra and T. K. Rusch. Enhancing accuracy of deep learning algorithms by training with low-discrepancy sequences. *SIAM Journal on Numerical Analysis*, 59(3):1811–1834, 2021.
- [24] H. Niederreiter. *Random Number Generation and Quasi-Monte Carlo Methods*. S.I.A.M., Philadelphia, PA, 1992.
- [25] E. Novak and H. Wozniakowski. *Tractability of multivariate problems*, volume II: standard information for functionals. European Mathematical Society, Zurich, 2010.
- [26] A. B. Owen. *Practical Quasi-Monte Carlo*. At <https://artowen.su.domains/mc/practicalqmc.pdf>, 2023.
- [27] F. Pausinger and A. M. Svane. A koksma–hlawka inequality for general discrepancy systems. *Journal of Complexity*, 31(6):773–797, 2015.
- [28] T. K. Rusch, N. Kirk, M. M. Bronstein, C. Lemieux, and D. Rus. Message-Passing Monte Carlo: Generating low-discrepancy point sets via graph neural networks. *Proceedings of the National Academy of Sciences*, 121(40):e2409913121, 2024.
- [29] I. H. Sloan and S. Joe. *Lattice Methods for Multiple Integration*. Oxford Science Publications, Oxford, 1994.
- [30] I. H. Sloan and H. Wozniakowski. When are quasi-Monte Carlo algorithms efficient for high dimensional integration? Technical report, University of New South Wales, School of Mathematics, 1997.
- [31] J. G. van der Corput. Verteilungsfunktionen I. *Nederl. Akad. Wetensch. Proc.*, 38:813–821, 1935.
- [32] J. G. van der Corput. Verteilungsfunktionen II. *Nederl. Akad. Wetensch. Proc.*, 38:1058–1066, 1935.
- [33] T. T. Warnock. Computational investigations of low-discrepancy point sets. In *Applications of number theory to numerical analysis*, pages 319–343. Elsevier, 1972.

- [34] H. Weyl. Über ein problem aus dem gebiete der diophantischen approximationen. *Nachrichten der Akademie der Wissenschaften in Göttingen. II. Mathematisch-Physikalische Klasse*, pages 234–244, 1914.
- [35] H. Weyl. Über die gleichverteilung von zahlen mod. eins. *Mathematische Annalen*, 77:313–352, 1916.
- [36] S. K. Zaremba. Some applications of multidimensional integration by parts. *Annales Polonici Mathematici*, 21:85–96, 1968.
- [37] Y.-D. Zhou, K.-T. Fang, and J.-H. Ning. Mixture discrepancy for quasi-random point sets. *Journal of Complexity*, 29(3):283–301, 2013.

A Additional Empirical Results

Measure / n	16		32	
	Opt.	Sobol’	Opt.	Sobol’
Center	0.0216	0.0319	0.122	0.0194
Symmetric	0.0176	0.0317	0.0103	0.0172
Extreme	0.0159	0.0192	0.0088	0.0161
Periodic	0.0381	0.0411	0.0208	0.0234
Avg. Squared	0.0275	0.0358	0.0149	0.0217
Star	0.0253	0.0478	0.0136	0.0212
Mixture	0.0413	0.0511	0.0218	0.0289

Measure / n	64		128		256	
	Opt.	Sobol’	Opt.	Sobol’	Opt.	Sobol’
Center	0.0068	0.0093	0.0036	0.0054	0.0020	0.0039
Symmetric	0.0057	0.0105	0.0033	0.0059	0.0018	0.0033
Extreme	0.0049	0.0111	0.0027	0.0052	0.0015	0.0028
Periodic	0.0114	0.0131	0.0060	0.0089	0.0034	0.0052
Avg. Squared	0.0082	0.0174	0.0043	0.0069	0.0023	0.0043
Star	0.0075	0.0101	0.0041	0.0059	0.0022	0.0045
Mixture	0.0120	0.0139	0.0062	0.0084	0.0034	0.0057

Table 3: D_2^\bullet discrepancy values for $\bullet \in \{*, \text{ctr}, \text{per}, \text{sym}, \text{ext}, \text{asd}, \text{mix}\}$ of MPMC point sets trained under the respective measure, and equivalent discrepancy value for Sobol’.

n / Measure	*	asd	mix	ctr	per	sym	ext
10	0.0398	0.0421	0.0589	0.0307	0.0585	0.0269	0.0589
20	0.0211	0.0222	0.0325	0.0178	0.0329	0.0149	0.0325
30	0.0145	0.0163	0.0225	0.0128	0.0217	0.0111	0.0225
40	0.0116	0.0122	0.0177	0.0098	0.0171	0.0087	0.0177
50	0.0094	0.0100	0.0138	0.0083	0.0140	0.0071	0.0138
60	0.0080	0.0084	0.0116	0.0069	0.0120	0.0061	0.0116
70	0.0069	0.0070	0.0099	0.0062	0.0106	0.0054	0.0099
80	0.0061	0.0066	0.0092	0.0055	0.0094	0.0048	0.0092
90	0.0057	0.0059	0.0084	0.0049	0.0086	0.0044	0.0084
100	0.0050	0.0053	0.0074	0.0044	0.0077	0.0040	0.0074
110	0.0046	0.0047	0.0069	0.0040	0.0071	0.0037	0.0069
120	0.0045	0.0045	0.0063	0.0037	0.0066	0.0034	0.0063

Table 4: Optimal discrepancy values for several measures optimized by MPMC for two dimensions, $n = 10, 20, \dots, 120$.